

SPIN TUNNELING IN CONDUCTING OXIDES (invited)

Alexander BRATKOVSKY

Hewlett-Packard Laboratories, 3500 Deer Creek Road, Palo Alto, CA 94304-1392,
alexbr@hpl.hp.com

ABSTRACT

Direct tunneling in ferromagnetic junctions is compared with impurity-assisted, surface state assisted, and inelastic contributions to a tunneling magnetoresistance (TMR). Theoretically calculated direct tunneling in iron group systems leads to about a 30% change in resistance, which is close to experimentally observed values. It is shown that the larger observed values of the TMR might be a result of tunneling involving surface polarized states. We find that tunneling via resonant defect states in the barrier radically decreases the TMR (down to 4% with Fe-based electrodes), and a resonant tunnel diode structure would give a TMR of about 8%. With regards to inelastic tunneling, magnons and phonons exhibit opposite effects: one-magnon emission generally results in spin mixing and, consequently, reduces the TMR, whereas phonons are shown to enhance the TMR. The inclusion of both magnons and phonons reasonably explains an unusual bias dependence of the TMR.

The model presented here is applied qualitatively to half-metallics with 100% spin polarization, where one-magnon processes are suppressed and the change in resistance in the absence of spin mixing on impurities may be arbitrarily large. Even in the case of imperfect magnetic configurations, the resistance change can be a few 1000 percent. Examples of half-metallic systems are $\text{CrO}_2/\text{TiO}_2$ and $\text{CrO}_2/\text{RuO}_2$, and an account of their peculiar band structures is presented. The implications and relation of these systems to CMR materials which are nearly half-metallic, are discussed.

INTRODUCTION

Tunnel magnetoresistance (TMR) in ferromagnetic junctions, first observed more than a decade ago,^{1,2} is of fundamental interest and potentially applicable to magnetic sensors and memory devices.³ This became particularly relevant after it was found that the TMR for 3d magnetic electrodes reached large values at room temperature^{4,5}, and junctions demonstrated a non-volatile memory effect. These observations have ignited a world-wide effort towards using this effect in various applications, with memories and sensors being the most natural choices.

A simple model for spin tunneling has been formulated by Julliere¹ and further developed in Refs.^{6,7}. This model is expected to work rather well for iron, cobalt, and nickel based metals, according to theoretical analysis⁶ and experiments.⁴ However, it disregards important points such as impurity-assisted and inelastic scattering, tunneling into surface states, and the reduced effective mass of carriers inside the barrier. These effects are important for proper understanding of the behavior of actual devices, like peculiarities in their I-V curves, as considered in Ref.⁸ and the present paper. I shall also discuss a couple of half-metallic systems which should in principle achieve the ultimate magnetoresistance at room temperatures and low fields.

ELASTIC AND INELASTIC TUNNELING MODEL

The model that we will consider below includes a Hamiltonian for non-interacting conducting spin-split electrons H_0 , electron-phonon interaction H_{ep} , and exchange interaction with localized d_1 electrons H_x , the latter giving rise to the electron-magnon interaction. Impurities will be described by a short-range confining potential V_i ,

$$\begin{aligned} H &= H_0 + H_{ep} + H_x + H_i; \\ H_i &= \sum_{n_i} V_i(\mathbf{r} - \mathbf{r}_{n_i}) \end{aligned} \quad (1)$$

where \mathbf{r} stands for the coordinate of the electron and n_i denotes the impurity sites.

The non-interacting part of the Hamiltonian H_0 describes electrons in the ferromagnetic electrodes and insulating barrier according to the Schrodinger equation⁷

$$(H_{00} - \hbar^2 \nabla^2) \psi = E \psi; \quad (2)$$

where $H_{00} = (\hbar^2/2m) \nabla^2 + U$ is the single-particle Hamiltonian with $U(\mathbf{r})$ the potential energy, $h(\mathbf{r})$ the exchange energy ($= 0$ inside the barrier), σ stands for the Pauli matrices; indices $\sigma = 1, 2$, and 3 mark the quantities for left terminal, barrier, and right terminal, respectively (H_0 is the expression in brackets). We shall also use the following notations to clearly distinguish between left and right terminal: $p = k_1$ and $k = k_3$. Solution to this problem in the limit of a thick barrier provides us with the basis functions for electrons in the terminals and barrier to be used in Bardeen's tunneling Hamiltonian approach.^{9,10} We assume that all many-body interactions in the electrodes are included in the effective parameters of (2). To fully characterize tunneling we add to Bardeen's term H_T^0 the contributions from H_x and H_{ep} :

$$H_T = H_T^0 + H_T^x + H_T^{ep}; \quad (3)$$

$$H_T^0 = \sum_{p,k,a} T_{pa,ka}^0 r_{ka}^\dagger l_{pa} + h.c.;$$

$$T_{pa,ka}^0 = \frac{\hbar^2 (2m_2)}{2\pi} \int dA_{ka} \exp(i\mathbf{r}_{pa} - i\mathbf{r}_{ka}) \exp(i\mathbf{r}_{ka} - i\mathbf{r}_{pa}); \quad (4)$$

$$H_T^x = \sum_{n,k,p} T_{kp}^x(n) (S_n^3 - \hbar S_n^3 i) (r_{kp}^\dagger l_{p\#} - r_{k\#}^\dagger l_{p\#}) + S_n^+ r_{k\#}^\dagger l_{p\#} + S_n^- r_{k\#}^\dagger l_{p\#} + h.c.;$$

$$H_T^{ep} = \sum_{n,k,p} T_{kp}^{ep}(q) r_{ka}^\dagger l_{pa} (b_q^\dagger - b_q) + h.c.; \quad (5)$$

Here the surface Σ lies somewhere in the barrier and separates the electrodes, we have subtracted an average spin $S_n^3 - \hbar S_n^3 i$ in each of electrodes as part of the exchange potential, the exchange vertex is $T_{kp}^x = J_n \exp(-\mathbf{r}_{kp})$, and the phonon vertex is related to the deformation potential D in the usual way $[T_{kp}^{ep}(q) = D q (\hbar/2M \omega_q)^{1/2} \exp(-\mathbf{r}_{kp})]$, where M is the atomic mass, q is the phonon momentum, n marks the lattice sites, and the vertices contain the square root of the barrier transparency.^{10,11} The operators l_a and r_a annihilate electrons with spin a on the left and right electrodes, respectively. Two more things to note: (i) the summations over p and k always include density of initial g_{La} and final g_{Rb} states, that makes an exchange and phonon contribution spin-dependent, (ii) when the magnetic moments on the electrodes are at a mutual angle θ , one has to express the operator \mathbf{r} w.r.t. the lab system and then use it in H_T (5).

The tunnel current will be calculated within the linear response formalism as¹⁰

$$I(V;t) = \frac{e}{h} \int_{-\infty}^{\infty} dt \langle H_T(t) N_L(t) \rangle_0 \quad (6)$$

where $N_L(t) = \sum_{p_a} c_{p_a}^\dagger(t) c_{p_a}(t)$ is the operator of the number of electrons on the left terminal in the interaction representation, $\langle \dots \rangle_0$ stands for the average over H_0 ,

$$H_T(t) = \exp(-iVt/\hbar) A(t) + \text{h.c.}; \quad A(t) = \sum_{p_a, k_b} T_{p_a, k_b}(t) c_{k_b}^\dagger(t) c_{p_a}(t);$$

the tunnel vertex T is derived for each term in (5), and V is the bias. We shall later consider impurity-assisted tunneling within the same general approach.

Elastic tunneling

We are now in position to calculate all contributions to the tunneling current, the simplest being direct elastic tunneling due to H_T^0 . It is worth noting that it can also be calculated from the transmission probabilities of electrons with spin σ , $T_a = \sum_b T_{ab}$, is the transmission probability, which has a particularly simple form for a square barrier and collinear [parallel (P) or antiparallel (AP)] moments on the electrodes⁸ We obtain the following expression for the direct tunneling conductance, assuming $m_1 = m_3$ (below the effective mass in the barrier will be measured in units of m_1):

$$\frac{G^0}{A} = \frac{1}{A} \frac{I}{V} \Big|_{V \rightarrow 0} = G_{\text{FBF}}^0 (1 + P_{\text{FB}}^2 \cos(\theta)); \quad (7)$$

$$G_{\text{FBF}}^0 = \frac{e^2}{h} \frac{1}{w} \frac{m_2(U_0 - E_F) \left(\frac{1}{2} + m_2^2 k_\sigma k_\# \right)}{\left(\frac{1}{2} + m_2^2 k_\sigma^2 \right) \left(\frac{1}{2} + m_2^2 k_\#^2 \right)} e^{2\theta w}; \quad \text{and} \quad (8)$$

$$P_{\text{FB}} = \frac{k_\sigma - k_\#}{k_\sigma + k_\#} \frac{\frac{1}{2} - m_2^2 k_\sigma k_\#}{\frac{1}{2} + m_2^2 k_\sigma k_\#}; \quad (9)$$

where P_{FB} is the effective polarization of the ferromagnetic (F) electrode in the presence of the barrier (B), $\theta = [2m_2(U_0 - E_F)\hbar^2]^{1/2}$, and U_0 is the top of the barrier. Eq. (7) corrects an expression derived earlier⁷ for the effective mass of the carriers in the barrier. By taking a typical value of $G/A = 4.5 \times 10^{-4} \text{ cm}^{-2}$ (Ref.⁴) $k_\sigma = 1.09 \text{ \AA}^{-1}$, $k_\# = 0.42 \text{ \AA}^{-1}$, $m_1 = 1$ (for itinerant d electrons in FeF) and a typical barrier height for Al_2O_3 (measured from the Fermi level) $U_0 - E_F = 3 \text{ eV}$, and the thickness $w = 20 \text{ \AA}$, one arrives at the following estimate for the effective mass in the barrier: $m_2 = 0.4$.¹³ These values give the renormalized polarization $P_{\text{FeB}} = 0.28$, down from the bulk value for iron $P_{\text{Fe}} = 0.4$ (Ref.^{3,4}) Note that neglect⁷ of the mass correction would make $P_{\text{FeB}} < 0$, and this is not corroborated by experimental evidence.

In the standard approximation of a rectangular shape the barrier height is $U_0 = \frac{1}{2}(\phi_L + \phi_R - eV)$ and this leads to a quick rise of the conductance with bias, $G^0(V) = G^0 + \text{const} \cdot V$ at small V (ϕ_L and ϕ_R are the work functions of the electrodes). In practice, the barrier parameters should be extracted from independent experiments, such as internal photoemission, etc., but here we are concerned with the generic behavior, where the present formalism is sufficient for qualitative and even semi-quantitative analysis. Since the barrier shape depends in a non-trivial manner on image forces, the calculations have been performed numerically with actual barrier shape at finite temperatures (Fig. 1).

We note that the (undesirable) downward renormalization of the polarization rapidly goes with diminishing effective carrier mass in the barrier. The renormalization is completely absent in half-metallic ferromagnets with $R_{\text{eff}} = 0$, as we shall discuss below.

We define the magnetoresistance as the relative change in contact conductance with respect to the change of mutual orientation of spins from parallel (G^P for $\theta = 0$) to antiparallel (G^{AP} for $\theta = 180^\circ$) as

$$MR = (G^P - G^{AP})/G^{AP} = 2P_{FB}P_{FB}^0/(1 - P_{FB}P_{FB}^0): \quad (10)$$

The most striking feature of Eqs. (3),(4) is that the MR tends to infinity for vanishing R_{eff} , i.e. when both electrodes are made of a 100% spin-polarized material ($P = P^0 = 1$), because of a gap in the density of states (DOS) for minority carriers up to their conduction band minimum $E_{CB\#}$. Then G^{AP} vanishes together with the tunnel probability, since there is a zero DOS at $E = E_{CB\#}$ for both spin directions.

Such half-metallic behavior is rare, but some materials possess this amazing property, most interestingly the oxides CrO_2 and Fe_3O_4 .¹⁴ These oxides have potential for future applications in combination with lattice-matching materials, as we shall illustrate below.

A more accurate analysis of the $I-V$ curve requires a numerical evaluation of the tunnel current for arbitrary biases and magnetic forces, and the results are shown in Fig. 1. The top panel in Fig. 1 shows $I-V$ curves for an iron-based F-B-F junction with the above-mentioned parameters. The value of TMR is about 30% at low biases and steadily decreases with increased bias. In a half-metallic case ($R_{\text{eff}} = 0$, Fig. 1, middle panel, where a threshold $eV_c = E_{CB\#} = 0.3 \text{ eV}$ has been assumed), we obtain zero conductance G^{AP} in the AP configuration at biases lower than V_c . It is easy to see that above this threshold, $G^{AP} \propto (V - V_c)^{5/2}$ at temperatures much smaller than eV_c .⁸ Thus, for $|V| < V_c$ in the AP geometry one has $MR = \infty$. In practice, there are several effects that reduce this MR to some finite value, notably an imperfect AP alignment of moments in the electrodes. However, from the middle and the bottom panels in Fig. 1 we see that even at 20° deviation from the AP configuration, the value of MR exceeds 3,000% within the half-metallic gap $|V| < V_c$, and this is indeed a very large value.

Impurity-assisted tunneling

An important aspect of spin-tunneling is the effect of tunneling through the defect states in the (amorphous) oxide barrier. Since the devices under consideration are very thin, their $I-V$ curves and MR should be very sensitive to defect resonant states in the barrier with energies close to the chemical potential, forming "channels" with the nearly periodic positions of impurities (Fig. 2).¹⁵ Generally, channels with one impurity (most likely to dominate in thin barriers) would result in a monotonous behavior of the $I-V$ curve, whereas channels with two or more impurities would produce intervals with negative differential conductance.¹⁵

Impurity-assisted spin tunneling at zero temperature (at non-zero T one should include an integration with the Fermi functions) has a resonant form^{15;8}

$$G_a = \frac{2e^2 X}{h} \frac{L_a R_a}{(E_i - E_a)^2 + \gamma^2}; \quad (11)$$

where $\gamma = \Gamma_L + \Gamma_R$ is the total width of the resonance given by the sum of the partial widths Γ_L (Γ_R) corresponding to electron tunneling from the impurity state at the energy

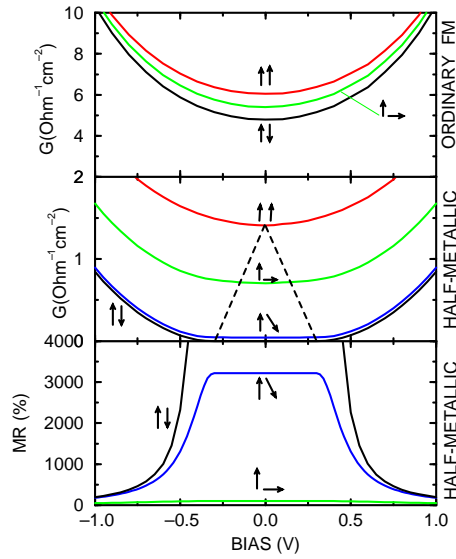


Figure 1: Conductance and magnetoresistance of tunnel junctions versus bias. Top panel: conventional (Fe-based) tunnel junction (for parameters see text). Middle panel: half-metallic electrodes. Bottom panel: magnetoresistance for the half-metallic electrodes. Dashed line shows schematically a region where a half-metallic gap in the minority spin states is controlling the transport. Even for imperfect antiparallel alignment ($\theta = 160^\circ$, marked "x"), the magnetoresistance for half-metallics (bottom panel) exceeds 3000% at biases below the threshold V_c . All calculations have been performed at 300K with the inclusion of multiple image potential and exact transmission coefficients. Parameters are described in the text.

E_i to the left (right) terminal. For the tunnel width we have

$$G_{(L,R)a} = \frac{2}{\pi} \frac{e^2}{h} \frac{(m_2^2)^2}{m_0^2} \sum_{k_{(L,R)a}} |j_{k_{(L,R)a}}(n_i)|^2 \delta(E_k - E_i); \quad (12)$$

where $j_{k_{(L,R)a}}(n_i)$ is the value of the electrode wave function, exponentially decaying into the barrier, at an impurity site n_i . For a rectangular barrier we have⁸

$$j_{La} = \frac{2m_2 k_a}{\pi} \frac{e^{-\kappa_0(w+2z_i)}}{\cosh^2(\frac{1}{2}\kappa_0 w + \kappa_0 z_i)}; \quad (13)$$

where z_i is the coordinate of the impurity with respect to the center of the barrier, $\kappa_0 = \sqrt{2m_2(E_i - E_F)}$. For e.g. P configuration and electrodes of the same material, the conductance would then be proportional to $\delta(E_i - E_F) + 4 \frac{m_2^2}{m_0^2} \cosh^2(\kappa_0 z_i)$, where κ_0 equals (13) without the factor $\exp(-\kappa_0 z_i)$ [c.f. Eq. (15)]. The conductance has a sharp maximum ($= e^2/h$) when $E_i = E_F$ and $\kappa_0 z_i = 0$, i.e. for the symmetric position of the impurity in the barrier $|z_i| < 1/\kappa_0$ in a narrow interval of energies $|E_i - E_F| < \hbar^2 \kappa_0^2 / 2m_2$. Averaging over energies and positions of impurities in Eq. (11), and considering a general configuration of the magnetic moments on the terminals, we get the following formula for impurity-assisted conductance in the leading order in $\exp(-\kappa_0 w)$:

$$\frac{G^1}{A} = G_{imp}^1 (1 + \frac{2}{F_B} \cos(\theta)); \quad (14)$$

where we have introduced the quantities

$$G_{imp}^1 = \frac{e^2}{h} N_1; \quad N_1 = \sum_{i=0}^{\infty} \frac{1}{1 + \kappa_0^2 z_i^2};$$

$$N_1 = \frac{e}{\hbar} \frac{0W}{0W} (r_{\#} + r_{\#})^2; \quad \Gamma_{FB} = (r_{\#} - r_{\#}) = (r_{\#} + r_{\#}); \quad \text{and} \\ r_a = [m_2^2 k_a^2 = (\frac{2}{0} + m_2^2 k_a^2)]^{1/2}; \quad (15)$$

with N_1 being the effective number of one-impurity channels per unit area, and Γ_{FB} is the 'polarization' of the impurity channels. When the total number of one-impurity channels $N_1 = N_1 A \gg 1$, then we will have a self-averaged conductance, otherwise the conductance will depend on a specific arrangement of impurities (regime of mesoscopic fluctuations).

Comparing the direct and the impurity-assisted contributions to conductance, we see that the latter dominates when the impurity density of states $\rho_0 = \frac{1}{\hbar} \exp(-0W)$, and in our example a crossover takes place at $10^7 \text{ cm}^{-3} \text{ eV}^{-1}$. When the resonant transmission dominates, the magnetoresistance is given by

$$MR_1 = 2 \frac{\rho_0}{\rho_0} (1 - \frac{\rho_0}{\rho_0}); \quad (16)$$

which is just 4% in the case of Fe. Thus, we have a drastic reduction of the TMR due to non-magnetic impurities in the tunnel barrier, and in the case of magnetic impurities the TMR will be even smaller.

With standard ferromagnetic electrodes, the conductance is exponentially enhanced $[G^1 / \exp(-0W)]$, whereas $G^0 \propto \exp(-20W)$ but the magnetoresistance is reduced in comparison with the 'clean' case of a low concentration of defect levels. These predictions⁸ have been confirmed by recent experiments.^{12,16}

With further increase of the defect density and/or the barrier width, the channels with two- and more impurities will become more effective than one-impurity channels described above, as has been known for quite a while.^{17,15} The contribution of the many-impurity channels, generally, will result in the appearance of irregular intervals with negative differential conductance on the $I-V$ curve.¹⁵ Thus, the two-impurity channels define random fluctuations of current with bias. This is due to the fact that the energy of defect states depends on bias as $\epsilon_i = \epsilon_i^0 + eVz/w$. With increasing bias (i) the total number of two-impurity channels increases but (ii) some of these channels go off resonance and reduce their conductance. Accidentally, the number of two-impurity channels going off resonance may become larger than a number of new channels, leading to suppressed overall conductance. If we denote by ϵ_2 the width of the two-impurity channels, then the fluctuations would obviously occur on a scale $V < \epsilon_2 = e$. Then, according to standard arguments, the change in current will be

$$\frac{\Delta I}{I} = \frac{V}{V} \frac{eV}{\epsilon_2} N_2^{-1/2}; \quad (17)$$

where $N_2 = eV N_2 / \epsilon_2$ is the number of the two-impurity channels contributing at the bias $V > \epsilon_2 = e$, N_2 is the total number of the two-impurity channels, $N_2 = A^3 w^3 \frac{2}{2} \frac{2}{0}^1$, and $\epsilon_2 = (4 \epsilon_1^2 = (\hbar 0W))^2$.¹⁵ When $eV = \epsilon_2 > N_2 (\hbar 0W)^2$, then the second (random) term in (17) exceeds the first term, and this leads to random intervals with negative differential conductance. Obviously, with increasing temperature or/and bias in thick enough barriers, longer and longer impurity channels will be 'turned on'. A corresponding microscopic model should include impurity states coupled to a phonon bath, and such a model has been solved in Ref.¹⁸. The authors found an average conductance due to an n -impurity chain in the limit $eV \gg T$, which gives for $n = 2$ $G_2(T) \propto T^{4/3}$. In the opposite limiting case of $eV \ll T$, the result is:¹⁸ $G_2(V) \propto V^{4/3}$, and this crossover behavior is indeed in very good agreement with experiments on a-Si barriers.¹⁹

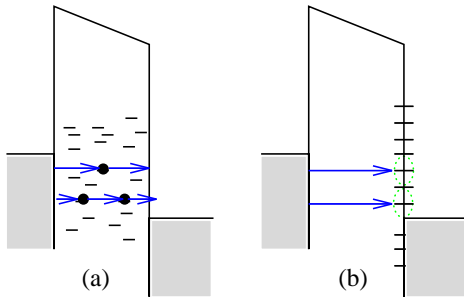


Figure 2: Schematic of tunneling via chains of the localized states in the barrier (a) and into the localized surface states (b).

One may try to fabricate a resonant tunnel diode (RTD) structure to sharply increase the conductance of a system. We can imagine an RTD structure with an extra thin non-magnetic layer placed between two oxide barrier layers producing a resonant level at some energy E_r . The only difference from the previous discussion is the effectively 1D character of the transport in the RTD in comparison with 3D impurity-assisted transport. However, the transmittance will have the same resonant form as in (11) and the widths (13). The estimated magnetoresistance in the RTD geometry is, with the use of (11),

$$M R_{\text{RTD}} = \frac{h}{(r_n^2 - r_\#^2)} = (2r_n r_\#)^{-1}; \quad (18)$$

which is about 8% for Fe electrodes. We see that the presence of random impurity levels or a single resonant level reduces the value of the magnetoresistance as compared with direct tunneling.

Roughness

As we have seen, the conductance is dominated by the exponentially small barrier transparency, $\propto \exp(-2w(\frac{1}{2} + k_k^2)^{1/2})$, so that the contribution comes mainly from electrons tunneling perpendicular to the barrier, i.e. with small parallel momenta $|k_k| < (\frac{1}{2}w)^{1/2}$. For barriers with a rough interface $w = \bar{w} + h$, where h is the height of asperities and \bar{w} is the average barrier thickness. Each asperity will contribute a factor of $\exp(2\frac{1}{2}h)$ to the conductance, which we have to average. We assume a normal distribution for roughness, $P(h) = (2h_0^2)^{-1/2} \exp(-h^2/(2h_0^2))$. Then, the average conductance \bar{G} becomes

$$\bar{G} = \int_0^\infty G dh \exp(2\frac{1}{2}h) P(h) = \bar{G} \exp(\frac{1}{2}h_0^2) / \exp[2\frac{1}{2}(\bar{w} + h_0^2)]: \quad (19)$$

This result means that the effective thickness of the barrier is reduced by h_0^2 in comparison with the observed average thickness \bar{w} . The generalization for the case of correlated roughness is straightforward and does not change this result.

Tunneling via Surface States

Direct tunneling, as we have seen, gives MR of about 30%, whereas the recent experimental results are almost ten percent higher.^{12;22} As we shall see shortly, this moderate difference is unlikely to come from the inelastic processes. Up to now we have disregarded the possibility of localized states at metal-oxide interfaces. Keeping in mind that the usual barrier AD_x

is an orphous, the density of such states may well exceed that at typical semiconductor-oxide surfaces. If this is true, then we have to take into account tunneling into/from those states. If we assume that electrons at the surface are confined by a short-range potential then we can estimate the tunneling matrix elements as described above. The corresponding tunneling M R is given by

$$\begin{aligned}\frac{G_{bs}(\omega)}{A} &= \frac{e^2}{h} \overline{D}_s (1 + P_{FB} P_s \cos(\theta)); \\ P_s &= \frac{D_{s''} - D_{s\#}}{D_{s''} + D_{s\#}}; \\ \overline{D}_s &= \frac{1}{2} (D_{s''} + D_{s\#}); \\ B &= 8 \frac{2}{0W} \frac{m_2 \omega (k'' + k_{\#}) (\frac{\omega^2}{2} + m_2^2 k'' k_{\#})}{(\frac{\omega^2}{2} + m_2^2 k''^2) (\frac{\omega^2}{2} + m_2^2 k_{\#}^2)} \exp(-2\omega W); \quad (20)\end{aligned}$$

where P_s is the polarization and \overline{D}_s is the average density of surface states, $\omega_s = \hbar^2 \omega^2 / (2m_2)$. The corresponding magnetoresistance would be $M R_{bs} = 2P_{FB} P_s / (1 - P_{FB} P_s)$.

Comparing (20) with (7), we see that the bulk-to-surface conductance exceeds bulk-to-bulk tunneling at moderate densities of surface states $D_s > D_{sc} \approx 10^{13} \text{ cm}^{-2} \text{ eV}^{-1}$ per spin.

If on both sides the density of surface states is above critical value D_{sc} , the magnetoresistance will be due to surface-to-surface tunneling with a value given by

$$M R_{ss} = 2P_{s1} P_{s2} / (1 - P_{s1} P_{s2});$$

and if the polarization of surface states is larger than in the bulk, then it would result in enhanced TMR. This mechanism may be even more relevant for Fe/Si and other ferromagnet-semiconductor structures.²⁰

INELASTIC TUNNELING, ZERO-BIAS' ANOMALY

So far we have disregarded all inelastic processes, such as phonon emission by the tunneling electrons. These processes were long thought to be responsible for a so-called 'zero-bias' anomaly observed in a variety of non-magnetic²¹ and magnetic junctions.^{12,22} Magnetism in electrodes introduces new peculiarities into the problem, which we will now discuss. The obvious one is related to emission of magnons. At temperatures well below the Curie temperature and not very large biases, one can describe spin excitations by introducing magnons. Then the calculations of exchange- and phonon-assisted currents become very similar. Thus, we obtain from (6) and (5) the following expression for magnon-assisted current in e.g. parallel conformation (corresponding expressions can be easily found for other conformations as well):

$$\begin{aligned}I_p^x(V; T) &= \frac{2eX}{h} \sum_q g_n^L g_{\#}^R (eV + \hbar\omega) \frac{N_{\#}}{1 - \exp(-\hbar\omega / k_B T)} + \frac{N_{\#} + 1}{1 - \exp(-\hbar\omega / k_B T)} \\ &+ g_{\#}^L g_n^R (eV - \hbar\omega) \frac{N_{\#} + 1}{1 - \exp(-\hbar\omega / k_B T)} + \frac{N_{\#}}{1 - \exp(-\hbar\omega / k_B T)}; \quad (21)\end{aligned}$$

where $N_{\#} = [\exp(\hbar\omega / k_B T) - 1]^{-1}$, $\hbar\omega = \hbar\omega_q$ and X is the magnon incoherent vertex related to the $J_{p\#}^{x;}$ $(2S_n = N)^{1/2} J$ (5) with all momenta parallel to

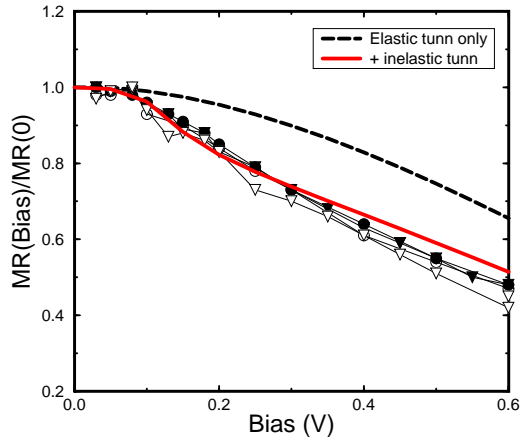


Figure 3: Fit to experimental data for the magnetoresistance of $\text{Co}/\text{Al}_2\text{O}_3/\text{NiFe}$ tunnel junctions [12] with inclusion of elastic and inelastic (magnons and phonons) tunneling. The fit gives for magnon DOS $\propto \omega^{0.65}$ which is close to the standard spectrum $\propto \omega^{1/2}$.

the barrier integrated out.¹¹ To get this expression, we have also assumed that the electron densities of states g in (21) vary on a larger scale than the bosonic contributions do, and, therefore, substituted them by representative values at the nominal Fermi levels. If there are some fine features in the electron DOS, then the integral over electron energies should remain, thus necessarily smoothing out any such fine features in the electron DOS.

For the limiting case of $T = 0$, we obtain for inelastic tunneling current:

$$\begin{aligned} I_P^x &= \frac{2eX}{h} \int_0^Z g_{\#}^L g_{\#}^R d\omega \theta^{\text{mag}}(\omega) (\text{eV} - \omega) (\text{eV} + \omega); \\ I_{AP}^x &= \frac{2e}{h} \int_0^Z g_{\#}^L g_{\#}^R d\omega \theta_R^{\text{mag}}(\omega) (\text{eV} - \omega) (\text{eV} + \omega) \\ &\quad + \int_0^Z g_{\#}^L g_{\#}^R d\omega \theta_L^{\text{mag}}(\omega) (\text{eV} - \omega) (\text{eV} + \omega); \end{aligned} \quad (22)$$

where $\theta(x)$ is the step function, $\theta^{\text{mag}}(\omega)$ is the magnon density of states that has a general form $\theta^{\text{mag}}(\omega) = (\omega + 1)\omega^{\alpha-1}$, can be used as a fitting parameter to define a dispersion of the relevant magnons, and ω_0 is the maximum magnon frequency. For phonon-assisted current at $T = 0$ we have

$$I_P^{\text{ph}} = \frac{2eX}{h} \int_0^Z g_a^L g_a^R d\omega \theta^{\text{ph}}(\omega) P(\omega) (\text{eV} - \omega) (\text{eV} + \omega); \quad (23)$$

$$I_{AP}^{\text{ph}} = \frac{2eX}{h} \int_0^Z g_a^L g_a^R d\omega \theta^{\text{ph}}(\omega) P(\omega) (\text{eV} - \omega) (\text{eV} + \omega); \quad (24)$$

One can show that the ratio of phonon to exchange vertex is $P(\omega) = X = \omega/\omega_D$, where X is a constant depending on the ratio between deformation potential and exchange constants,¹¹ and ω_D is the Debye frequency.

The elastic and inelastic contributions together will define the total junction conductance $G = G(V; T)$ as a function of the bias V and temperature T . We find that the inelastic contributions from magnons and phonons (22)–(24) grow as $G^{\text{mag}}(V; 0) \propto (eV \mp \omega_0)^{\alpha+1}$ and $G^{\text{ph}}(V; 0) \propto (eV \mp \omega_D)^4$ at low biases. These contributions saturate at higher biases:

$G^x(V;0) / 1 \sim \frac{+1}{+2} \frac{!_0}{\text{eV}} j$ at $j > !_0$; $G^{\text{ph}}(V;0) / 1 \sim \frac{4}{5} \frac{!_D}{\text{eV}} j$ at $j > !_D$. This behavior would lead to sharp features in the $I-V$ curves on a scale of 30-100 mV (Fig. 3).

It is important to highlight the opposite effects of phonons and magnons on the TMR. If we take the case of the same electrode materials and denote $D = g_{\uparrow}$ and $d = g_{\downarrow}$ then we see that $G_P^x(V;0) = G_{AP}^x(V;0) / (D - d^2)(\text{eV} - !_0)^{-1} < 0$, whereas $G_P^{\text{ph}}(V;0) = G_{AP}^{\text{ph}}(V;0) / (D - d^2)(\text{eV} - !_D)^{-4} > 0$, i.e. spin-mixing due to magnons kills, whereas the phonons tend to enhance the TMR.²³

Finite temperature gives contributions of the same respective sign as written above. For magnons: $G_P^x(0;T) = G_{AP}^x(0;T) / (D - d^2)(T - M = dT) < 0$, where $M = M(T)$ is the magnetic moment of electrode at given temperature T . Phonon contribution is given by standard Debye integral with the following results: $G_P^{\text{ph}}(0;T) = G_{AP}^{\text{ph}}(0;T) / (D - d^2)(T - !_D)^{-4} > 0$ at $T < !_D$, and linear temperature dependence at high temperatures $G_P^{\text{ph}}(0;T) = G_{AP}^{\text{ph}}(0;T) / (D - d^2)(T - !_D)$ at $T > !_D$.¹¹ We note again an opposite effect of magnons and phonons on the tunneling magnetoresistance.

We have not included Kondo²⁴ and other correlation effects that might contribute at very low biases, since they usually do not help to quantitatively fit the data.¹⁹

The role of phonons is illustrated by my fit to recent experiments carried out at HPL:¹² it appears that only after including phonons is it possible to get a sensible fit to the magnon DOS with $\alpha = 0.65$, which is close to the bulk value $\frac{1}{2}$ and $\beta = 0.1$ (Fig. 3).

100% POLARIZATION

It is very important that in the case of half-metallics $r_{\downarrow} = 0$, $r_{\text{FB}} = 1$, and even with an imperfect barrier magnetoresistance can, at least in principle, reach any value limited by only spin- $\uparrow\downarrow$ processes in the barrier/interface and/or misalignment of moments in the half-metallic ferromagnetic electrodes.⁸ We should note that the one-magnon excitations in half-metallics are suppressed by the half-metallic gap, as immediately follows from our discussion in the previous section. Spin-mixing can only occur on magnetic impurities in the barrier or interface, because the allowed two-magnon excitations in the electrodes do not result in spin-mixing.

Therefore, these materials should combine the best of both worlds: very large magnetoresistance with enhanced conductance in tunnel MR junctions. One should be aware, however, that defect states (like unpaired electrons) will increase the spin- $\uparrow\downarrow$ rate, so the magnetoresistance could vanish with an increasing concentration of defects. In the case of conventional systems (e.g. FeN electrodes) we have seen, however, that resonant tunneling significantly reduces the tunnel MR by itself, so the possibility of improving the conductance and still having a very large magnetoresistance resides primarily with half-metallics. I shall finish with a couple of examples of systems with half-metallic behavior, $\text{CrO}_2/\text{TiO}_2$ and $\text{CrO}_2/\text{RuO}_2$ ⁸ (Fig. 4). They are based on half-metallic CrO_2 , and all materials have the rutile structure with almost perfect lattice matching, which should yield a good interface and should help in keeping the system at the desired stoichiometry. TiO_2 and RuO_2 are used as the barrier/spacer oxides. The half-metallic behavior of the corresponding multilayered systems is demonstrated by the band structures calculated within the linear muffin-tin orbitals method (LMTO) in a supercell geometry with [001] growth direction and periodic boundary conditions. The calculations show that $\text{CrO}_2/\text{TiO}_2$ is a perfect half-metallic, whereas $(\text{CrO}_2)_2/\text{RuO}_2$ is a weak half-metallic, since there is some small DOS around E_F , and an exact gap opens up at about 0.58 eV above the Fermi level (Fig. 4). In comparison, there are only states in the majority spin band at the Fermi level in $\text{CrO}_2/\text{TiO}_2$. An immediate

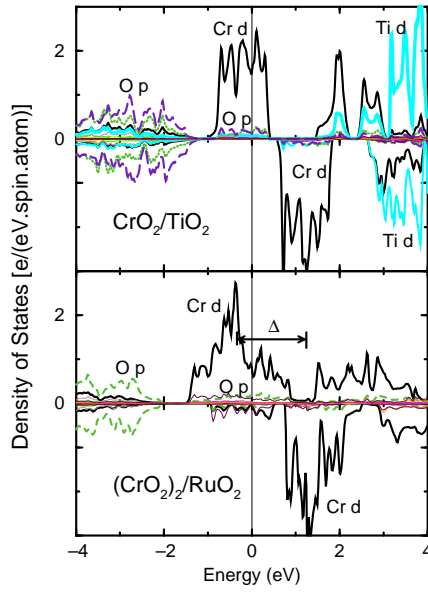


Figure 4: Density of states of $\text{CrO}_2/\text{TiO}_2$ (top panel) and $(\text{CrO}_2)_2/\text{RuO}_2$ (bottom panel) half-metallic layered structures calculated with the use of the LMTO method.

consequence of the fact that minority spin bands are fully occupied is an exact integer value of the magnetic moment in the unit cell ($= 2 \mu_B/\text{Cr}$ in $\text{CrO}_2/\text{TiO}_2$), and this property is a simple check for possible new half-metallics.

The electronic structure of $\text{CrO}_2/\text{TiO}_2$ is very interesting in that it has a half-metallic gap which is 2.6 eV wide and extends on both sides of the Fermi level, where there is a gap either in the minority or majority spin band. Thus, an huge magnetoresistance should in principle be seen not only for electrons at the Fermi level biased up to 0.5 eV, but also for hot electrons starting at about 0.5 eV above the Fermi level. We note that states at the Fermi level are a mixture of Cr(d) and O(2p) states, so that p-d interaction within the first coordination shell produces a strong hybridization gap, and the Stoner spin-splitting moves the Fermi level right into the gap for minority carriers (Fig. 4).

An important difference between the two spacer oxides is that TiO_2 is an insulator whereas RuO_2 is a good metallic conductor. Thus, the former system can be used in a tunnel junction, whereas the latter will form a metallic multilayer. In the latter case the physics of conduction is different from tunneling but the effect of vanishing phase volume for transmitted states still works when current is passed through such a system perpendicular to planes. For the P orientation of moments on the electrodes, $\text{CrO}_2/\text{RuO}_2$ would have a normal metallic conduction, whereas in the AP one we expect it to have a semiconducting type of transport, with a crossover between the two regimes. One interesting possibility is to form three-terminal devices with these systems, like a spin-valve transistor,²⁵ and check the effect in the hot-electron region. $\text{CrO}_2/\text{TiO}_2$ seems to be a natural candidate to check the present predictions about half-metallic behavior and for a possible large tunnel magnetoresistance. An important advantage of these systems is almost perfect lattice matching at the oxide interfaces. The absence of such a match of the conventional Al_2O_3 barrier with Heusler half-metallics (NMnSb and PtMnSb) may have been among other reasons for their moderate performance.²⁶

By using all-oxide half-metallic systems, as described herein, one may bypass many materials issues. Then, the main concerns for achieving a very large value of magnetoresistance

will be spin- \uparrow centers and imperfect alignment of moments. As for conventional tunnel junctions, the present results show that the presence of defect states in the barrier, or a resonant state like in a resonant tunnel diode type of structure, reduces their magnetoresistance by several times but may dramatically increase the current through the structure.

Finally, we can mention the CMR materials. Experiment²⁷ and LDA calculations²⁸ indicate that manganites are close to half-metallic behavior as a result of a significant spin-splitting presumably due to strong Hund's rule coupling on Mn. Manganites are strongly correlated materials, likely with electronic phase separation,²⁹ which makes their study a real challenge. There are a number of studies of systems, where transport is going across grain boundaries or between MnO_2 layers in tailored derivatives of the perovskite phase.³⁰ A hope is that some of these structures with manganites might operate at low fields and reasonably high temperatures.³¹ The low field (below 1000 Oe) TMR in polycrystalline $\text{La}_{2/3}\text{Sr}_{1/3}\text{MnO}_3$ perovskite and $\text{Tl}_2\text{Mn}_2\text{O}_7$ pyrochlore is about 30% and is likely due to intergrain carrier transport. It would be interesting to apply the results of the present work to tunneling phenomena in the CMR-based layered/inhomogeneous structures. For instance, CrO_2 junctions would help to check on the relevance of the half-metallic behavior to conduction in the CMR materials. In particular, it should be signalled by a plateau in the tunneling magnetoresistance as a function of bias within the half-metallic band gap (Fig. 1).

I am grateful to J. Nickel, T. Anthony, J. Brug, and J. Moodera for sharing their data, and to G. A. D. Briggs, N. Moll, and R. S. Williams for useful discussions.

REFERENCES

1. M. Julliere, Phys. Lett. 54A, 225 (1975).
2. S. Maekawa and U. Gafvert, IEEE Trans. Magn. 18, 707 (1982).
3. R. Meservey, P. M. Tedrow, Phys. Reports 238, 173 (1994).
4. J. S. Moodera et al., Phys. Rev. Lett. 74, 3273 (1995); J. Appl. Phys. 79, 4724 (1996).
5. T. Miyazaki and N. Tezuka, J. Magn. Mater. 139, L231 (1995).
6. M. B. Steams, J. Magn. Mater. 5, 167 (1977); Phys. Rev. B 8, 4383 (1973).
7. J. C. Slonczewski, Phys. Rev. B 39, 6995 (1989).
8. A. M. Bratkovsky, Phys. Rev. B 56, 2344 (1997); JETP Lett. 65, 452 (1997).
9. J. Bardeen, Phys. Rev. Lett., 6, 57 (1961).
10. G. D. Mahan, Many-Particle Physics, 2nd ed., Plenum, New York, 1990, Ch. 9; C. B. Duke, Tunneling in Solids, Academic Press, New York, 1969, Ch. 7.
11. A. M. Bratkovsky (to be published).
12. J. Nickel, T. Anthony, and J. Brug, private communication.
13. Q. Q. Shu and W. G. Ma, Appl. Phys. Lett. 61, 2542 (1992) give even smaller $m_2 = 0.2$ for $\text{Al-Al}_2\text{O}_3$ -metal junctions.
14. V. Y. Irkhin and M. I. Katsnelson, Sov. Phys. - Uspekhi 164, 705 (1994).
15. A. I. Larkin and K. A. Matveev, Zh. Eksp. Teor. Fiz. 93, 1030 (1987); I. M. Lifschitz and V. Ya. Kirpichenkov, Zh. Eksp. Teor. Fiz. 77, 989 (1979).
16. R. Jansen and J. S. Moodera (1997), to be published.
17. M. Pollak and J. J. Hauser, Phys. Rev. Lett. 31, 1304 (1973); A. V. Tartakovskii et al., Sov. Phys. Semicond. 21, 370 (1987); E. I. Levin et al., Sov. Phys. Semicond. 22, 401 (1988); J. B. Pendry, J. Phys. C 20, 733 (1987).
18. L. I. Glazman and K. A. Matveev, Sov. Phys. JETP 67, 1276 (1988).
19. Y. Xu, D. Ephron, and M. Beasley, Phys. Rev. B 52, 2843 (1995).

20. A. Chaiken, R. P. Michel, and M. A. Wall, Phys. Rev. B 53, 5518 (1996).
21. C. B. Duke, S. D. Silverstein, and A. J. Bennett, Phys. Rev. Lett. 19, 315 (1967).
22. J. Moodera, private communication.
23. In a recent attempt to explain the $I-V$ curves of ferromagnetic junctions S. Zhang et al (1997, preprint) have apparently neglected a strong bias dependence of the direct tunneling and did not consider the effect of phonons.
24. J. Appelbaum, Phys. Rev. Lett. 17, 91 (1966).
25. D. J. Monsma et al, Phys. Rev. Lett. 74, 5260 (1995).
26. C. T. Tanaka and J. S. Moodera, J. Appl. Phys. 79, 6265 (1996).
27. Y. Okimoto et al, Phys. Rev. B 55, 4206 (1997); Phys. Rev. Lett. 75, 109 (1995).
28. W. E. Pickett and D. J. Singh, Phys. Rev. B 53, 1146 (1996); D. J. Singh, Phys. Rev. B 5, 313 (1997).
29. G. Allodi et al. Phys. Rev. B 56, 6036 (1997); E. L. Nagaev, JETP Lett. 6, 484 (1967); Phys. Rev. B 54, 16608 (1996); *ibid.* 56, 14583 (1997).
30. M. K. Gubkin et al. Phys. Sol. State 35, 728 (1993); H. Y. Hwang et al, Phys. Rev. Lett. 77, 2041 (1996); J. Z. Sun et al, Appl. Phys. Lett. 69, 3266 (1996); T. Kimura et al, Science 274, 1698 (1996).
31. H. Y. Hwang and S. W. Cheong, Science 389, 942 (1997).